On the Estimation of SAR and Compliance Distance Related to RF Exposure From Mobile Communication Base Station Antennas

Björn Thors, Marie L. Strydom, *Member, IEEE*, Björn Hansson, Frans J. C. Meyer, Kimmo Kärkkäinen, Peter Zollman, Sami Ilvonen, and Christer Törnevik, *Member, IEEE*

***Abstract*—In this paper, maximum specific absorption rate (SAR) estimation formulas for RF main beam exposure from mobile communication base station antennas are proposed. The formulas, given for both whole-body SAR and localized SAR, are heuristic in nature and valid for a class of common base station antennas. The formulas were developed based on a number of physical observations and are supported by results from an extensive literature survey together with supplementary measurements and numerical simulations of typical exposure situations. Using exposure limits, the proposed SAR estimation formulas can be converted to formulas for estimating compliance distance.**

***Index Terms*—Electromagnetic field exposure, finite-difference time-domain (FDTD) methods, mobile communication base station antennas, moment methods, specific absorption rate.**

I. Introduction

When new mobile communication base station products are placed on the market and put into service, it is important for manufacturers and operators to make sure that the RF electromagnetic exposure is in compliance with appropriate safety standards and regulations. In most countries, the safety guidelines published by the International Commission on Non-Ionizing Radiation Protection (ICNIRP) [1] have been adopted. Different regional compliance assessment standards are available, e.g., [2], and an international standard is currently being developed by the International Electrotechnical Commission (IEC 62232) [3].

Human exposure is usually quantified in terms of the specific absorption rate (SAR), which is the time derivative of dissipated energy per unit mass within the exposed body due to the incident electromagnetic fields. For frequencies between 100 kHz and 10 GHz, basic restrictions on SAR are provided to prevent established adverse health effects related to whole-body heat stress and excessive localized tissue heating. ICNIRP's basic restrictions on whole-body SAR[1] and localized SAR[2] are given in [1].

For practical exposure assessment purposes, ICNIRP also specifies frequency-dependent reference levels to determine whether the basic restrictions may be exceeded. The reference levels for mobile communication frequencies are expressed in terms of an equivalent plane wave with limit values for electric field strength, magnetic field strength, and power density. These quantities are assessed in free space and are often used to determine compliance boundaries[3] around base station antennas. In deriving the reference levels, differences in absorption of electromagnetic energy by individuals of different sizes and different orientations relative to the field were taken into account by ICNIRP, including effects of reflection, focusing and scattering of the incident field to establish a maximum coupling condition between the field and the exposed person. Compliance with the reference levels should ensure compliance with the basic restrictions [1].

A drawback with using reference levels for exposure assessment is that this tends to overestimate compliance distances since in real near-field exposures, the incident field is not a plane wave and maximum coupling conditions may not apply. Using basic restrictions produces more accurate compliance distances but requires experimental or analytical methods that are more sophisticated in order to take the interaction between the field and the human body into account, see, e.g., [4]–[6]. In [7] and [8], two heuristic compliance distance estimation formulas, based on numerical SAR simulations, were proposed to generate compliance distances and to simplify the adherence process. The proposed formulas were developed for a class of 2100-MHz wideband code-division multiple access (WCDMA) base station antennas. This idea was later expanded on in [9], where the formula was evaluated against previously published results.

In this paper, a more detailed investigation has been made and estimation formulas for whole-body and localized SAR

Manuscript received April 16, 2007; revised February 19, 2008. Current version published November 20, 2008.

B. Thors, B. Hansson, and C. Törnevik are with Ericsson Research, KI/EAB/TF, SE-164 80 Stockholm, Sweden (e-mail: bjorn.thors@ericsson.com).

M. L. Strydom was with EMSS Consulting, Stellenbosch 7600, South Africa. She is now with CST Gmbh, D-64289 Darmstadt, Germany.

F. J. C. Meyer is with EMSS Consulting, Stellenbosch 7600, South Africa (e-mail: fjcmeyer@emss.co.za).

K. Kärkkäinen was with Nokia Corporation, Nokia Group, FI-00045 Espoo, Finland. He is now with Equal Dreams Ltd., FI-02150 Espoo, Finland.

P. Zollman is with Vodafone Group R&D, The Connection, Newbury RG14 2FN, U.K. (e-mail: peter.zollman@vodafone.com).

S. Ilvonen is with Helsinki University of Technology, FI-02150 Espoo, Finland (e-mail: sami.ilvonen@tkk.fi).

Color versions of one or more of the figures in this paper are available online at http://ieeexplore.ieee.org.

Digital Object Identifier 10.1109/TEMC.2008.2004605

[1]SAR averaged over the total body mass, in this paper abbreviated $\mathrm{SAR}_{\mathrm{wb}}$.

[2]Maximum value of SAR averaged over 10 g of contiguous tissue, in this work abbreviated $\mathrm{SAR}_{10\mathrm{g}}$.

[3]The compliance boundary defines a volume outside of which the exposure levels do not exceed a certain limiting value, irrespective of the time of exposure. Compliance boundaries can be defined both in terms of reference levels and in terms of basic restrictions. The distance from the antenna to the outermost part of the compliance boundary defines the compliance distance.

are proposed for a class of common base station antennas. The use of estimation formulas in terms of SAR, instead of compliance distance, has the advantage of not being dependent on a particular set of exposure limits. Besides avoiding cumbersome numerical simulations or measurements, the SAR estimation formulas also produce shorter and more accurate compliance distances compared with methods based on the reference levels. The proposed formulas were developed based on an extensive literature survey with results from both measurements [10]–[13] and simulations [7], [8], [14]–[24]. Supplementary measurements, using a DASY4 near-field scanner, and numerical simulations, using the commercial electromagnetic solvers FEKO (hybrid Finite Element/Moment Method) and SEMCAD (Finite Difference Time Domain), have been performed. In the simulations, various antenna types were considered together with the full-body phantoms, namely, Zubal (heterogenous) [25], [26], visible human male (heterogenous) [27], Norman (heterogeneous) [28], Seth Seidman[4] (heterogeneous), and specific anthropomorphic mannequin (homogeneous) [29]. The measurements were performed in accordance with the European standard EN 50383 [2], and the procedure used in the numerical simulations is described in [30] and [31], which also contain some results.

In Section II, the SAR estimation formulas are developed and comparisons are made with published data and additional measurement and simulation results. Using ICNIRP's basic restrictions, the SAR estimation formulas are converted into formulas for compliance distance in Section III. In Section IV, some clarifying comments regarding necessary tradeoffs and the spread of the SAR data are made. Finally, in Section V some conclusions are given.

II. SAR Estimation Formulas

The purpose of this study was to develop whole-body and localized SAR estimation formulas for a class of commonly used base station antennas in order to facilitate RF exposure assessments. The formulas were developed to produce a conservative estimate for main beam exposure. Outside the main beam, the formulas will be even more conservative. Both groundplane-backed and horizontal omnidirectional antennas have been considered.

Guided by published data, measurements, and numerical simulation results, it is possible to heuristically define simple analytical expressions that will overestimate the SAR levels. In the following section, some physical observations are discussed that provide the framework for the proposed estimation formulas. Some restrictions are discussed in Section II-B while the formulas are presented in Section II-C. Comparisons with numerical and experimental results are shown in Section II-D.

A. Physical Observations

In the far-field region, the wave propagation is spherical in nature and the transmitted power density decays as $1/r^2$, where r is the distance from the antenna. Since the whole-body and localized SAR are proportional to the incident power density in the far-field region, the SAR estimation formulas should have the same distance dependence. In the radiating near-field region, the wave propagation is essentially cylindrical and the transmitted power density decays as $1/r$. The transition from cylindrical to spherical wave propagation is gradual, but for our overestimation formulas, we may assume

$$\mathrm{SAR}_{10\mathrm{g,wb}} \propto \begin{cases} \dfrac{1}{r}, & r'_{10\mathrm{g,wb}} \le r \le r''_{10\mathrm{g,wb}} \\ \dfrac{1}{r^2}, & r > r''_{10\mathrm{g,wb}}, \end{cases} \tag{1}$$

where $r'_{10\mathrm{g,wb}}$ and $r''_{10\mathrm{g,wb}}$ denote transition points between the different field regions as specified next.

The SAR values are directly related to the level of absorbed power. Outside the reactive near-field region, the beamwidths of the antenna play an increasingly important role for the levels of absorbed power. Narrower beamwidths will result in a higher power density thus increasing the SAR. With the lossy body placed close to the antenna, the absorbed power is more related to the fields surrounding the individual antenna elements.

When a human body is in close proximity to a base station antenna, coupling between the body and the individual elements may cause the input impedance to change, alter the array excitation, and change the radiated power [32]. For the quantities of interest in this paper, the largest impact will be on localized SAR. For separation distances smaller than $\lambda/4$, where λ denotes the wavelength, a $\mathrm{SAR}_{10\mathrm{g}}$ increase of up to 45% has been observed [13], [33].

Another factor that will affect the SAR levels is the number of antenna elements. By reducing the number of radiators the transmitted power will be distributed over fewer elements thus leading to a higher localized SAR for small human–antenna separations. The way the elements are situated in the array lattice will affect the SAR levels for larger separation distances.

In addition, the size of the exposed body will affect the SAR levels (primarily whole-body SAR). A smaller body will result in a higher whole-body SAR since the mass, roughly proportional to the body volume, is reduced at a faster rate compared with the absorbed power, roughly proportional to the cross-sectional area.

B. Restrictions

Truly useful estimation formulas should be simple, easy to implement, valid for a large class of antennas, and conservative if used to demonstrate compliance with exposure limits. Some of these requirements are conflicting and a tradeoff is therefore needed. With the data currently available, and as a consequence of this tradeoff, the following restrictions have been imposed.

1) The frequency range is limited to 800 MHz $\le f \le$ 2200 MHz. Supporting SAR data are available for the frequency range 900 MHz $\le f \le$ 2200 MHz, but since the 800 MHz mobile communication bands are within a few a percent from 900 MHz, similar antennas are used, and the level of energy absorption is continuous with respect to the frequency, it is reasonable to expect that the frequency range can be extended down to 800 MHz.

[4]The Seth Seidman phantom was supplied by Dr. Wolfgang Kainz at the US Food and Drug Administration.

2) The whole-body SAR data considered in this paper were obtained from numerical simulations with adult male phantoms. Hence, the proposed whole-body SAR formulas are expected to be valid for adult exposure.

C. Proposed Formulas

Based on the aforesaid physical observations and taking the restrictions into consideration, the following estimation formula is proposed for localized SAR valid for the head and trunk region

$$\mathrm{SAR}_{10\mathrm{g}}\left(r,P,N,\Phi,r'_{10\mathrm{g}},r''_{10\mathrm{g}}\right)=\begin{cases}\widetilde{A}\widetilde{B}\dfrac{P}{Nr'_{10\mathrm{g}}} & r<r'_{10\mathrm{g}}\\ \widetilde{B}\dfrac{P}{N\Phi r}, & r'_{10\mathrm{g}}\le r\le r''_{10\mathrm{g}}\\ \widetilde{B}\dfrac{Pr''_{10\mathrm{g}}}{N\Phi r^2}, & r>r''_{10\mathrm{g}},\end{cases} \tag{2}$$

where P, N, and Φ denote the transmitted power, the number of antenna elements,[5] and the horizontal half-power beamwidth,[6] respectively. The constants $\widetilde{A}$ and $\widetilde{B}$ are given by

$$\widetilde{A} = \frac{3}{2} \tag{3}$$

$$\widetilde{B} = 1\mathrm{m}\cdot\mathrm{kg}^{-1} \tag{4}$$

where $\widetilde{A}$ is introduced to account for a possible increase in localized SAR for small human–antenna separations, as discussed in Section II-A (observed maximum increase of 45%), and the value of $\widetilde{B}$, corresponding to the vertical alignment of the curve, is chosen to obtain a good fit with the available data. The breakpoint distance $r'_{10\mathrm{g}}$ is chosen as[7]

$$r'_{10\mathrm{g}} = \frac{\lambda}{4} \tag{5}$$

corresponding to the commonly used distance to define the boundary between the reactive and the radiating near-field regions for base station antennas, see, e.g., [2]. From [35], the breakpoint distance $r''_{10\mathrm{g}}$, separating the regions of cylindrical and spherical wave propagation, is chosen as

$$r''_{10\mathrm{g}} = \frac{\Phi}{12}D_0L \tag{6}$$

where Φ, D_0, and L denote the horizontal half-power beamwidth, the broadside directivity, and the length of the antenna, respectively.

The corresponding SAR estimation formula for limb exposure is obtained by multiplying the head and trunk formula with a factor of two. This factor is based on observations made when calculating localized SAR in, e.g., the hands.

[5]In this context, N should be interpreted as the number of elements producing unique and well-defined localized SAR maxima for small antenna-phantom separations. As a rule of thumb, neighboring elements are counted individually if the separation distance is larger than $\lambda/4$ (center to center).

[6]In the estimation formulas, the beamwidth should be expressed in radians. For antennas with more than one major lobe, e.g., a bidirectional antenna, Φ should be taken as the sum of the individual half-power beamwidths.

[7]For one-element antennas, it is more appropriate to choose the breakpoint distance as $r'_{10\mathrm{g}} = 0.6\sqrt{L^3/\lambda}$, where L denotes the length of the antenna [34].

The proposed estimation formula for whole-body SAR is given by

$$\mathrm{SAR}_{\mathrm{wb}}\left(r,P,\Phi,r'_{\mathrm{wb}},r''_{\mathrm{wb}}\right)=\begin{cases}\widetilde{C}\,P, & r<r'_{\mathrm{wb}}\\ \widetilde{D}\dfrac{P}{\Phi r}, & r'_{\mathrm{wb}}\le r\le r''_{\mathrm{wb}}\\ \widetilde{D}\dfrac{Pr''_{\mathrm{wb}}}{\Phi r^2}, & r>r''_{\mathrm{wb}}\end{cases} \tag{7}$$

where

$$\widetilde{C} = \frac{1}{75}\ \mathrm{kg}^{-1} \tag{8}$$

$$\widetilde{D} = \frac{1}{200}\ \mathrm{m}\cdot\mathrm{kg}^{-1}. \tag{9}$$

By choosing the breakpoint distance r'_{wb} as

$$r'_{\mathrm{wb}} = \frac{\widetilde{D}}{\widetilde{C}\Phi} \tag{10}$$

a good fit with the published data and the experimental and numerical results was obtained. The breakpoint distance r''_{wb}, selected to be consistent with the far-field formula and ICNIRP's reference levels, can be written as

$$r''_{\mathrm{wb}}=\begin{cases}\widetilde{E}\dfrac{D_0\Phi}{\pi f}, & 800\,\mathrm{MHz}\le f<2000\,\mathrm{MHz}\\ \widetilde{F}\dfrac{D_0\Phi}{\pi}, & 2000\,\mathrm{MHz}\le f\le 2200\,\mathrm{MHz}\end{cases} \tag{11}$$

where

$$\widetilde{E} = 8\times 10^{8}\ \mathrm{m}\cdot\mathrm{s}^{-1} \tag{12}$$

$$\widetilde{F} = \frac{2}{5}\,\mathrm{m}. \tag{13}$$

D. Comparisons With Numerical and Experimental Results

Besides the physical foundation on which the estimation formulas are based, the largest support for the validity of the formulas comes from a comparison against the vast number of results obtained from published research papers and supplementary measurements and numerical simulations. In total, the estimation formulas have been verified against results from more than 120 different exposure assessments. In the following sections, the features of the estimation formulas are demonstrated for different kinds of exposure situations.

In the Appendix, some antenna-related parameters are given together with the corresponding breakpoint distances for the antennas used in the exposure assessments presented next. A transmitted power of 1 W has been assumed for all results presented in this section. For antenna–phantom separation distances larger than 10 m, the data points were obtained using a far-field approximation, in which the numerical phantoms were exposed to plane waves with the corresponding power densities normalized to distance and directivity [7].

In the numerical simulations, the effects of power redistribution among the array elements (for small antenna–phantom separations) were not included. For these exposure situations, it is therefore reasonable to expect a somewhat higher localized SAR in the reactive near-field region.

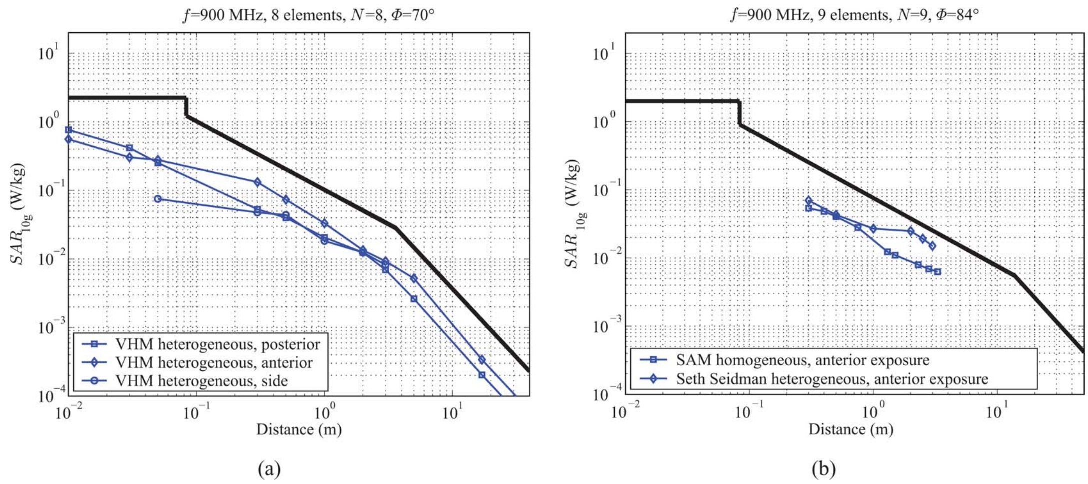

Fig. 1. Localized SAR results compared with the estimation formula (black solid line). (a) Eight-element array with groundplane transmitting at 900 MHz [30]. (b) Nine-element array with groundplane transmitting at 900 MHz [31].

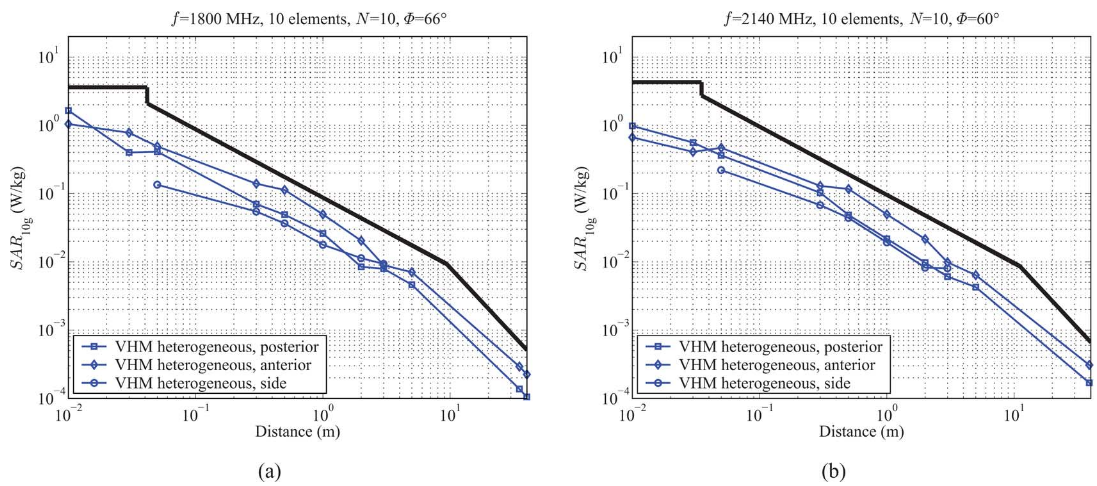

Fig. 2. Localized SAR results compared with the estimation formula (black solid line). (a) Ten-element array with groundplane transmitting at 1800 MHz [30]. (b) Ten-element array with groundplane transmitting at 2140 MHz [30].

1) Localized SAR: In Fig. 1, the estimation formula for localized SAR is compared against results obtained with two groundplane-backed 900-MHz base station antennas using three different whole-body numerical phantoms [30], [31]. As shown in Fig. 1(a), the formula adapts well to the easily discernible regions of cylindrical and spherical wave propagation.

In Fig. 2, similar comparisons are presented for a ten-element array operating at 1800 MHz and 2140 MHz, respectively [30].

The impact of the antenna size can be illustrated by comparing results from a ten-element array in Fig. 2(b) with Fig. 3(a), where the results were obtained using three different four-element arrays operating at 2140 MHz. Even though the horizontal half-power beamwidth is similar for the four arrays, the reduced length of the 4-element antennas causes the transition between cylindrical and spherical wave propagation to occur closer to the arrays. A consequence of the reduced number of elements is that higher SAR levels are obtained in the reactive and radiating near-field regions.

In Fig. 3(b), a comparison is shown for a two-column base station array antenna with 6×2 elements [22]. Due to the small horizontal element separation, the number of elements in (2) was taken as $N = 6$. For the two-column array in Fig. 4(a) (5×2 elements), the horizontal element separation is larger and $N = 10$ [21]. The larger horizontal element separation produces a narrower beam in the horizontal direction ($\Phi < 1\ \mathrm{rad} \approx 60^\circ$), and for these types of antennas, the simple estimation formula is more conservative for small separation distances in the region of cylindrical wave propagation. This is a consequence of the tradeoff made when designing the estimation formula for localized SAR. Since base station antennas with narrow horizontal beamwidths are not that common in practice, it was decided not to incorporate this effect into the formula in order to maintain its simplicity.

In Fig. 4(b), a comparison is shown for an omnidirectional array antenna. Due to the omnidirectional properties, rather low localized SAR levels are obtained in the radiating near-field and in the far-field region. As stated in Section II-A, in the reactive near-field region, localized SAR is more related to the individual antenna elements [cf. Fig. 2(a)]. Another comparison with an omnidirectional

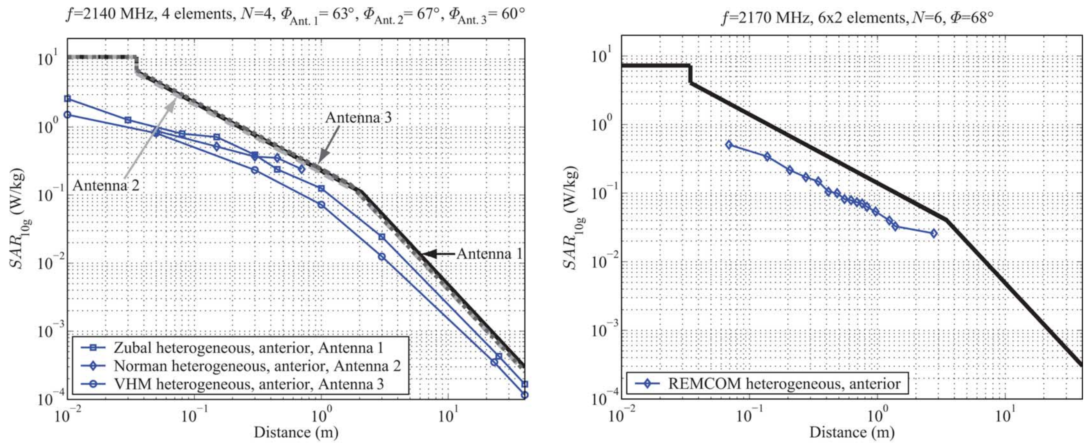

(a) (b)

Fig. 3. Localized SAR results compared with the estimation formula (black solid line). (a) Supplementary FDTD simulations, Three different four-element arrays with groundplane (denoted Antenna 1, Antenna 2, and Antenna 3, respectively) transmitting at 2140 MHz. (b) 6×2-element array with groundplane transmitting at 2170 MHz [22].

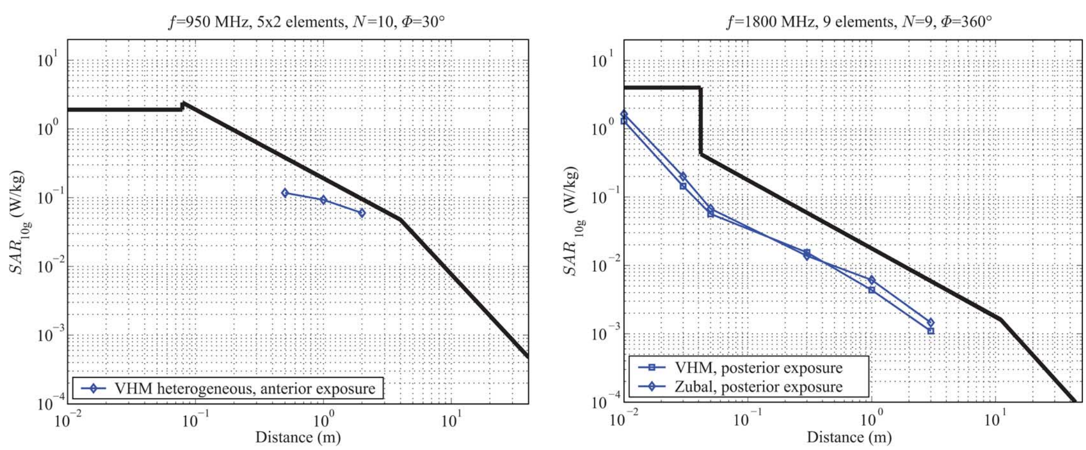

(a) (b)

Fig. 4. Localized SAR results compared with the estimation formula (black solid line). (a) 5×2-element array with groundplane transmitting at 950 MHz [21]. (b) Supplementary FDTD simulations, nine-element omnidirectional array transmitting at 1800 MHz.

antenna is shown in Fig. 5(a), where a 900 MHz dipole is considered.

In Fig. 5(b), a comparison with measured results is shown for a four-element base station antenna operating at 900 MHz. Note, the relative increase in localized SAR for small separation distances as a consequence of power redistribution between the antenna elements [cf. Fig. 5(a)].

2) Whole-Body SAR: In Fig. 6, the whole-body SAR estimation formula is compared against two sets of results, corresponding to two different antennas, obtained with four different numerical phantoms [30], [31]. Also, for whole-body SAR, the estimation formula adapts well to the different regions of cylindrical and spherical wave propagation, as shown in Fig. 6(a).

Corresponding comparisons for antennas transmitting at 900 and 2140 MHz, used in conjunction with the VHM, are shown in Fig. 7 [30]. A comparison of Fig. 7(b) with Figs. 8(a) and (b), where results are given for three smaller antennas transmitting at 2140 MHz [7], [36], illustrates the impact of antenna size. In the reactive near-field region, the estimation formula predicts a constant SAR value that compares well with the available data. The breakpoint distances, however, depend on the size of the antenna, both directly and indirectly via the directivity and the horizontal half-power beamwidth.

In Fig. 9, comparisons are shown for two different two-column base station array antennas [21], [22]. The relatively large difference in whole-body SAR for the two exposure situations is accounted for in the estimation formula via the horizontal half-power beamwidth in the denominator of (7) (cf. Table 1 in the Appendix).

In Fig. 10, the whole-body SAR estimation formula is compared against numerical results obtained for two omnidirectional antennas (one array and one single dipole) using two numerical phantoms.

III. Compliance Distance Estimation Formulas

Given a set of exposure limits, $\mathrm{SAR}^{\mathrm{lim}}_{10\mathrm{g,wb}}$, the SAR estimation formulas can be converted into formulas for compliance

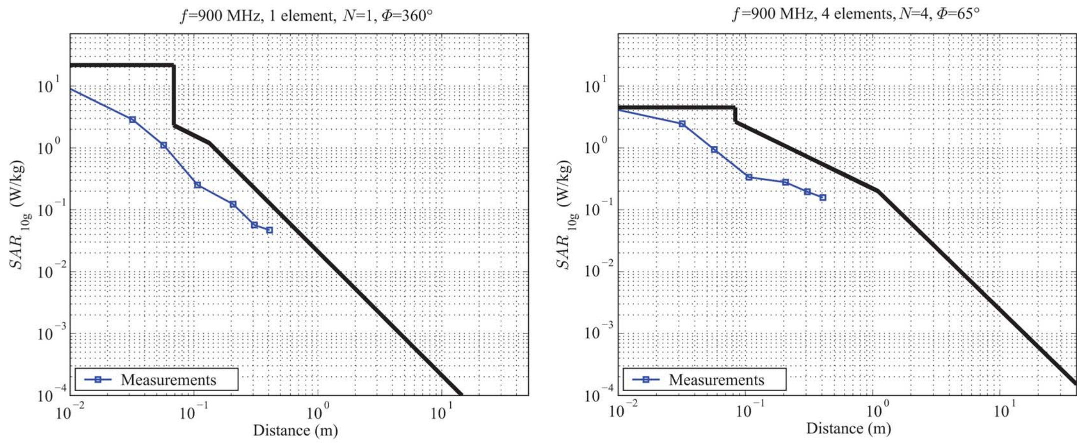

(a) (b)

Fig. 5. Localized SAR results compared with the estimation formula (black solid line). (a) Supplementary measurements, one-element omnidirectional antenna transmitting at 900 MHz (Racal 1640-923-100). (b) Supplementary measurements, four-element array with groundplane transmitting at 900 MHz (Kathrein 739620).

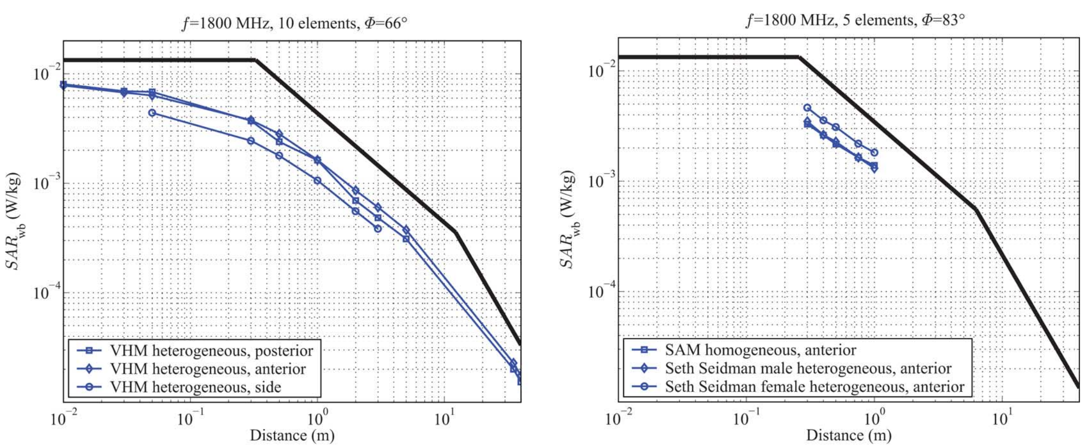

(a) (b)

Fig. 6. Whole-body SAR results compared with the estimation formula (black solid line). (a) Ten-element array with groundplane transmitting at 1800 MHz [30]. (b) Five-element array with groundplane transmitting at 1800 MHz [31].

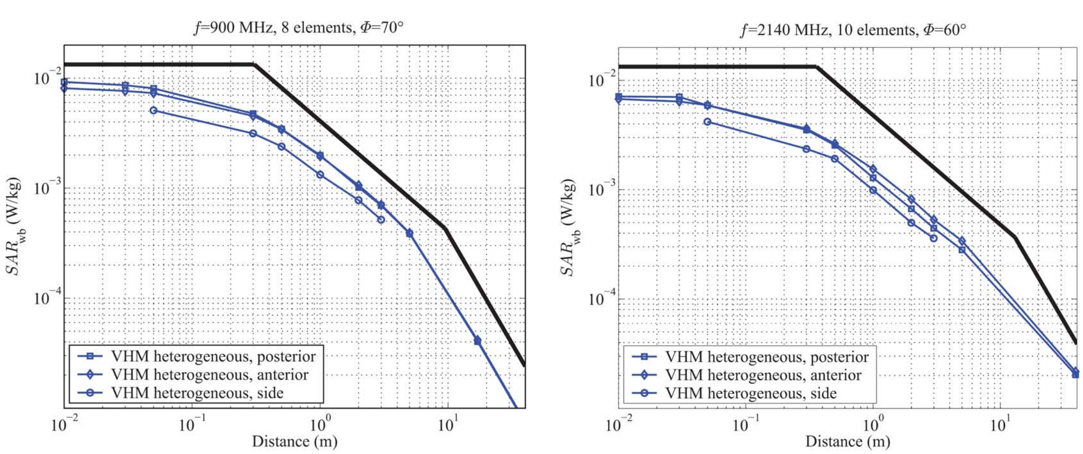

(a) (b)

Fig. 7. Whole-body SAR results compared with the estimation formula (black solid line). (a) Eight-element array with groundplane transmitting at 900 MHz [30]. (b) Ten-element array with groundplane transmitting at 2140 MHz [30].

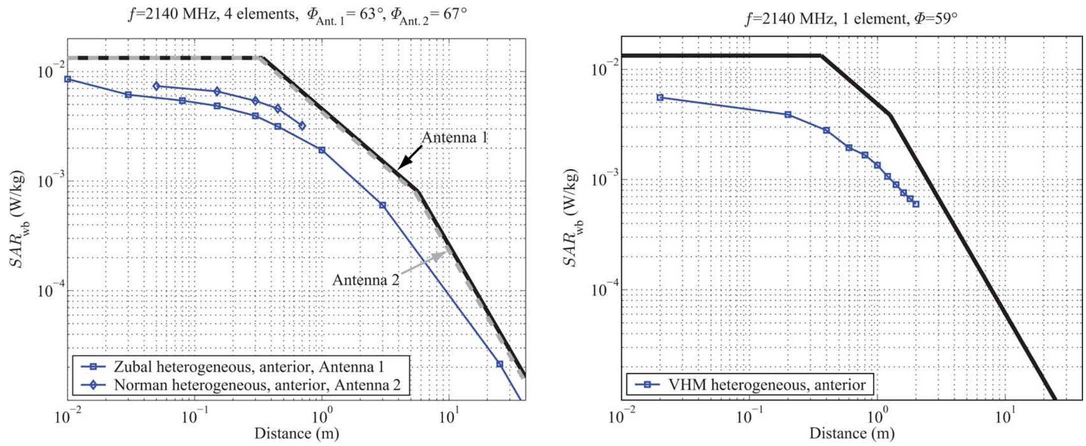

(a) (b)

Fig. 8. Whole-body SAR results compared with the estimation formula (black solid line). (a) Supplementary FDTD simulations, Two different four-element arrays with groundplane (denoted Antenna 1 and Antenna 2, respectively) transmitting at 2140 MHz. (b) One-element dipole with groundplane transmitting at 2140 MHz [7].

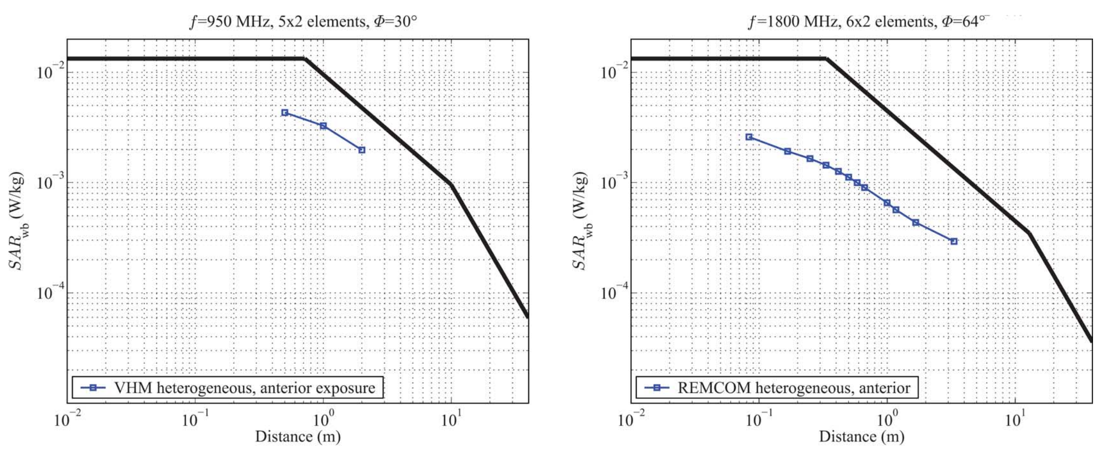

(a) (b)

Fig. 9. Whole-body SAR results compared with the estimation formula (black solid line). (a) 5×2-element array with groundplane transmitting at 950 MHz [21]. (b) 62-element array with groundplane transmitting at 1800 MHz [22].

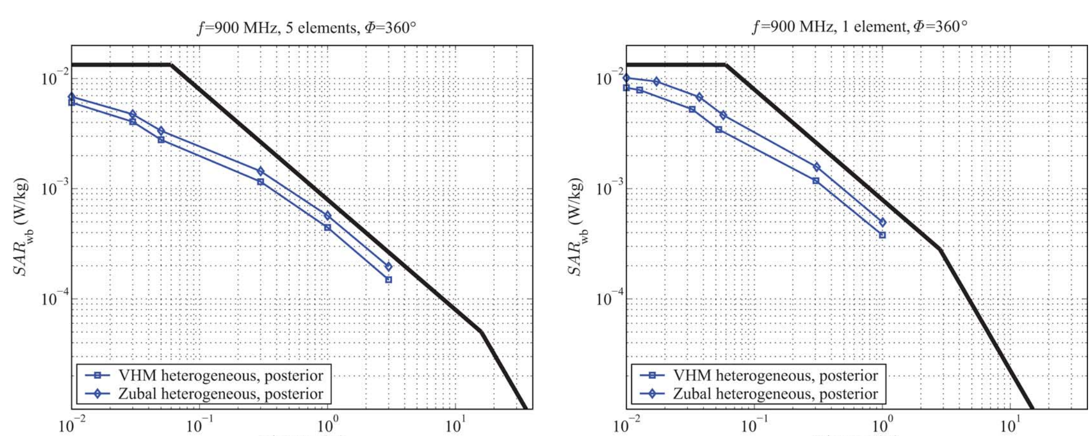

(a) (b)

Fig. 10. Whole-body SAR results compared with the estimation formula (black solid line). (a) Supplementary FDTD simulations, five-element omnidirectional antenna transmitting at 900 MHz. (b) Supplementary FDTD simulations, one-element omnidirectional antenna transmitting at 900 MHz.

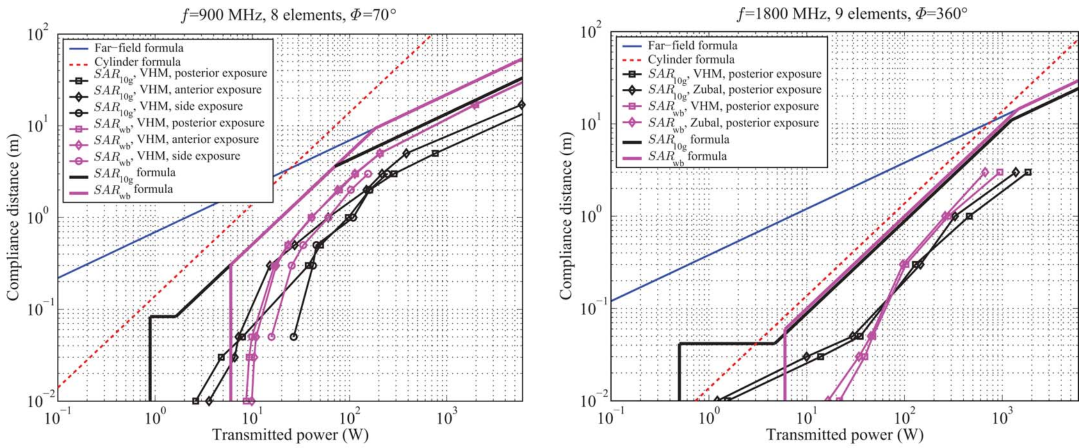

(a) (b)

Fig. 11. Compliance distance as a function of transmitted power. (a) Eight-element array with groundplane transmitting at 900 MHz [30]. (b) Supplementary FDTD simulations, nine-element omnidirectional antenna transmitting at 1800 MHz.

distance with the equation

$$P_{\mathrm{c}} = \frac{P\,\mathrm{SAR}^{\mathrm{lim}}_{10\mathrm{g,wb}}}{\mathrm{SAR}_{10\mathrm{g,wb}}\,(P, r_{\mathrm{c}})}, \tag{14}$$

where r_{c} denotes the compliance distance and P_{c} denotes the transmitted power producing a SAR value corresponding to the exposure limit.

This is illustrated in Fig. 11, where, using ICNIRP's basic restrictions [1], the compliance distance is plotted as a function of power for a groundplane-backed array antenna [30] and an omnidirectional array antenna, transmitting at 900 MHz and 1800 MHz, respectively. Shown also are comparisons against the cylinder formula[8]

$$S_{\mathrm{cyl}} = \frac{P}{L\Phi r} \tag{15}$$

and the far-field formula

$$S_{\mathrm{ff}} = \frac{PG}{4\pi r^2} \tag{16}$$

used in combination with ICNIRP's power density reference levels. In the aforesaid equations, S and G denote the power density and the antenna gain, respectively.

As shown in Fig. 11, the cylinder formula and the far-field formula overestimate the compliance distance compared with the SAR estimation formulas. The only exception is in the reactive near-field of the omnidirectional array (i.e., for these frequencies, within a few centimeters from the antennas), where the cylinder formula may predict a shorter compliance distance. In this region, however, the cylinder formula should not be used since the electric and magnetic field components must be treated separately. Localized SAR is in this region more related to the individual elements and the cylinder formula cannot always be expected to produce a conservative estimate of the compliance distance.

[8]For a more complete description of the cylinder formula, see [35] and [37]. In the case of (15), the average power density is estimated over a surface defined by the antenna length and half-power beamwidth [38].

The gain, by using the SAR estimation formulas compared with the cylinder formula, in terms of the reduced compliance distance, depends on the exposure situation. For the exposure situations analyzed in this study, the SAR estimation formulas predicted maximum compliance distances in the radiating near-field region that were approximately 35%–80% of the corresponding distances predicted with the cylinder formula.

Another consequence of the behavior of the SAR estimation formulas in the reactive near-field region is that they provide guidance on low-power exclusion, for which localized SAR is the limiting quantity.[9] As an example, for the special case considered in Fig. 11(b), it is evident that the omnidirectional array is unconditionally compliant with ICNIRP's basic restrictions if the transmitted power is less than 0.5 W.

IV. Discussion

The aim when developing the formulas was to incorporate as much physics as possible while keeping the formulas simple and easy to use. This tradeoff has led to some simplifications, and when plotted as a function of distance in a diagram with logarithmic scales, the formulas consist of a number of straight lines connected at different breakpoints. At the breakpoints, the derivatives of the SAR expressions with respect to the separation distance are discontinuous, which clearly is nonphysical. Since the estimation formulas were designed to be conservative, this was deemed to be acceptable in order to maintain the simplicity of the formulas. Another consequence of this tradeoff is that for some, in practice rarely used, narrow-beam base station antennas, the highest localized SAR may be predicted at the boundary between the reactive and the radiating near-field regions.

[9]For the most commonly used base station antennas, estimates of low-power exclusion limits are obtained by inserting the predicted value of localized SAR for the reactive near-field into (14). Special care is required for some narrow-beam antennas for which the estimation formula may predict the highest localized SAR at the boundary between the reactive and the radiating near-field regions [cf. Fig. 4(a)]. As mentioned in Section II-D, this is a consequence of the tradeoff made when designing the formulas.

TABLE I
ANTENNA-RELATED PARAMETERS USED IN THE EXPOSURE ASSESSMENTS PRESENTED IN SECTION II-D

Figure(s) no.	Antenna type	f (MHz)	No. of elem.	L (m)	Θ (deg.)	Φ (deg.)	D (dBi)
1(a), 7(a), 11(a)	Generic dipole array with groundplane [30]	900	8	1.3	12	70	14
1(b)	Generic dipole array with groundplane [31]	900	9	2.2	8.2	84	17
2(a), 6(a)	Generic dipole array with groundplane [30]	1800	10	1.3	7.2	66	19
2(b), 7(b)	Generic dipole array with groundplane [30]	2140	10	1.3	6.1	60	20
3(a), 8(a) Ant. 1/Ant. 2/Ant. 3	Generic dipole arrays with groundplane	2140/2140/2140	4/4/4	0.56/0.54/0.51	13/13/14	63/67/60	16/16/16
3(b)	Generic dipole array with groundplane [22]	2170	6x2	0.75	10	68	17
4(a), 9(a)	Generic dipole array with groundplane [21]	950	5x2	1.3	15	30	19
4(b), 11(b)	Generic omni-directional array	1800	9	1.3	6.8	omni	12
5(a)	Racal 1640-923-100	900	1	0.16	78	omni	2.0
5(b)	Kathrein 739620	900	4	0.66	27	65	13
6(b)	Generic dipole array with groundplane [31]	1800	5	0.66	14	83	15
8(b)	Generic dipole with groundplane [7]	2140	1	0.16	61	59	9.8
9(b)	Generic dipole array groundplane [22]	1800	6x2	0.9	10	64	19
10(a)	Generic omni-directional array	900	5	1.4	12	omni	9.5
10(b)	Generic dipole without groundplane	900	1	0.17	75	omni	2.0

The conservativeness of the formulas implies that they can easily be used to demonstrate compliance with exposure limits. The formulas should, however, not be used to show noncompliance since they have been developed as a conservative estimate. In order to have the same level of confidence for noncompliance, the data would need further evaluation to develop complementary noncompliance formulas. This would need to take into account the spread of the SAR data. For example, for the data considered in this study, the spread was obtained by calculating the fifth percentile of the variable $\mathrm{SAR}^{\mathrm{data}}/\mathrm{SAR}^{\mathrm{est.form.}}$, which equaled approximately -10.5 dB. In other words, 95% of the available SAR data points are located in the interval $[-10.5, 0]$ dB with respect to the estimation formulas. The remaining 5% are located below -10.5 dB.

The proposed estimation formulas were primarily developed for, and have to a certain extent been adjusted to, array antennas. Nevertheless, they also provide a conservative estimate of localized and whole-body SAR for single-element antennas.

Some of the supporting data were obtained for antennas with typical electrical tilt (up to 6°). In the near-field, right in front of the antenna, a few degrees of electrical tilt will not have a significant effect on localized and whole-body SAR. In the far-field, the formulas were designed to produce a conservative estimate for main beam exposure. To maintain the simplicity of the formulas, the tilt dependence was not included specifically.

Even though the formulas have been validated against a very large number of simulation and measurement results, it should be clear that the number of existing results is limited. Nevertheless, the proposed formulas have taken all the present available data into account, and as such, are reflecting the current state of knowledge. As the research progresses and more data become available for a wider set of antenna–phantom configurations, a refinement of the formulas may be made[10]. As mentioned earlier, the whole-body SAR data considered in this paper were obtained from numerical simulations with adult male phantoms. An interesting extension of the formulas would be to consider whole-body exposure of children and small women when data become available.

V. CONCLUSION

In this paper, conservative and efficient SAR estimation formulas for RF main beam exposure from base station antennas have been proposed. The formulas, although heuristic in nature,

[10] A major research study addressing this issue has recently been initiated by the Mobile Manufacturers Forum and the GSM Association.

are based on a set of physical observations and are supported by results from a large number of studies in the literature, as well as by supplementary measurements and numerical simulations. In total, the estimation formulas have been verified against results from more than 120 different exposure assessments.

By using exposure limits, the SAR estimation formulas can easily be converted into formulas for compliance distance. The resulting compliance distance estimators produce results that are more accurate compared with results obtained with methods based on reference levels, such as the cylinder and the far-field formulas.

The behavior of the SAR estimation formulas in the reactive near-field region implies that they can be used to provide guidance on low-power exclusion for antennas that are comprised by the formulas.

Appendix

Antenna-Related Parameters

In Table I, some antenna-related parameters are given for the antennas used in the exposure assessments presented in Sections II-D and III. Note that Θ denotes the vertical half-power beamwidth.

Acknowledgment

The authors would like to thank their colleagues from the IEC 62232 standardization project team for valuable comments. The authors would also like to thank Dr. W. Kainz and Dr. P. Dimbylow for providing the Seth Seidman and the Norman numerical phantoms, respectively.

References

[1] ICNIRP, "Guidelines for limiting exposure to time-varying electric, magnetic, and electromagnetic fields (up to 300 GHz)," *Health Phys.*, vol. 74, pp. 494–522, 1998.

[2] *Basic Standard for the Calculation and Measurement of Electromagnetic Field Strength and SAR Related to Human Exposure From Radio Base Stations and Fixed Terminal Stations for Wireless Telecommunication Systems (110 MHz to 40 GHz)*, CENELEC EN 50383, BTech. Committee 211, European Committee for Electrotechnique Standardization (CENELEC), Aug. 2002.

[3] *Determination of RF Fields in the Vicinity of Mobile Communication Base Stations for the Purpose of Evaluating Human Exposure*, IEC62232 Ed.1 CD, 2008.

[4] K. Poković, "Advanced electromagnetic probes for near-field evaluations," Ph.D. dissertation, Swiss Fed. Inst. Technol., 1999.

[5] Q. Balzano, O. Garay, and T. J. Manning, Jr, "Electromagnetic energy exposure of simulated users of portable cellular telephones," *IEEE Trans. Veh. Technol.*, vol. 44, no. 3, pp. 390–403, Aug. 1995.

[6] F. J. C. Meyer, D. B. Davidson, U. Jakobus, and M. A. Stuchly, "Human exposure assessment in the near field of GSM base-station antennas using a hybrid finite element/method of moments technique," *IEEE Trans. Biomed. Eng.*, vol. 50, no. 2, pp. 224–233, Feb. 2003.

[7] E. Nordström, "Calculation of specific absorption rate (SAR) for typical WCDMA base station antennas at 2140 MHz," Inst. Technol., Linköpings Univ., LinköpingTech. Rep., 2004.

[8] L. Hamberg, E. Nordström, and C. Törnevik, "FDTD calculation of SAR levels for typical 3G WCDMA base station antennas at 2140 MHz," in *Proc. BioEM*, 2005, pp. 70–73.

[9] F. Meyer and V. Kellerman, "Using SAR calculations and measurements for compliance zone assessment around base station antennas," in *Proc. BEMS*, 2006, p. 173.

[10] A. Bahr, D. Manteuffel, D. Gerhardt, and K. Menzel, "Occupational safety in the near field of GSM base stations," presented at the IEEE AP-S, Davos, Switzerland, Apr. 9–14 2000.

[11] W. Joseph and L. Martens, "Comparison of safety distances based on the electromagnetic field and based on the SAR for occupational exposure of a 900-MHz base station antenna," *IEEE Trans. Electromagn. Compat.*, vol. 47, no. 4, pp. 977–985, Nov. 2005.

[12] L. Hamberg, "SAR test report: Kathrein 738 446, KRE 101 1923/2," Ericsson Res., Tech. Rep., 2004.

[13] P. Håkansson, B. Thors, J. Danestig, B. Hansson, and C. Törnevik, "Effects on localized SAR of power redistribution between the antenna elements for loaded base station antennas," presented at the 29th Annu. Meeting Bioelectromagn. Soc., Jun. 2007, Kanazawa, Japan.

[14] J. Cooper, B. Marx, J. Buhl, and J. Hombach, "Determination of safety distance limits for a human near a cellular base station antenna, adopting the IEEE standard or ICNIRP guidelines," *Bioelectromagnetics*, vol. 23, pp. 429–443, 2002.

[15] P. Bernardi, M. Cavagnaro, S. Pisa, and E. Piuzzi, "Numerical evaluation of human exposure to radio base station antennas," presented at the XXVIIth URSI Gen. Assem., Maastricht, The Netherlands, Aug. 2002.

[16] P. Bernardi, M. Cavagnaro, S. Pisa, and E. Piuzzi, "Numerical evaluation of the compliance distance of radio base station antennas," presented at the 25th Annu. Meeting Bioelectromagn. Soc., Hawaii Island, HI, 2003.

[17] L. Catarinucci, P. Palazzari, and L. Tarricone, "Human exposure to the near field of radiobase antennas—a full wave solution using parallel FDTD," *IEEE Trans. Microw. Theory Tech.*, vol. 51, no. 3, pp. 935–940, Mar. 2003.

[18] O. P. Gandhi and M. S. Lam, "An on-site dosimetry system for safety assessment of wireless base stations using spatial harmonic components," *IEEE Trans. Antennas Propag.*, vol. 51, no. 4, pp. 840–847, Apr. 2003.

[19] F. J. C. Meyer, M. van Wyk, and R. Kellerman, "Compliance zone profiling of a commercial GSM base station antenna based on numerical SAR calculations," presented at the 27th Annu. Meeting Bioelectromagn. Soc., Dublin, Ireland, 2005.

[20] F. J. C. Meyer, M. van Wyk, and R. Kellerman, "Compliance zone profiling of a GSM base station antenna with the FEM/MoM," presented at the 16th Int. Zurich Symp. Electromagn. Compat., Geneva, Switzerland, 2005.

[21] V. Hansen, A. Bitz, J. Streckert, and A. El Ouardi, "A numerical approach for efficient calculation of human exposure in front of base station antennas," presented at the XXVIIIth URSI Gen. Assem., New Delhi, India, Oct. 2005.

[22] M. Martínez-Búrdalo, A. Martín, M. Anguiano, and R. Villar, "On the safety assessment of human exposure in the proximity of cellular communications base-station antennas at 900, 1800 and 2170 MHz," *Phys. Med. Biol.*, vol. 50, no. 17, pp. 4125–4137, Sep. 2005.

[23] F. Lacroux, A. Cortel Carrasco, A. Gati, M.-F. Wong, and J. Wiart, "SAR and averaged power density near a UMTS base-station antenna," presented at the 28th Annu. Meeting Bioelectromagn. Soc., Cancun, Mexico, 2006.

[24] S. Ilvonen, K. Kärkkäinen, T. Uusitupa, I. Laakso, and K. Nikoskinen, "Studying the accuracy of FDTD analysis for human exposure evaluations in the vicinity of a base station antenna," in *Proc. PIERS*, Beijing, China, Mar. 26–30, 2007, pp. 98–99.

[25] I. Zubal, C. Harrell, E. Smith, Z. Rattner, G. Gindi, and P. Hoffer, "Computerized three-dimensional segmented human anatomy," *Med. Phys.*, vol. 21, pp. 299–302, 1994.

[26] [Online]. Available: http://noodle.med.yale.edu/zubal/index.htm

[27] M. J. Ackerman, "The visible human project," *Proc. IEEE*, vol. 86, no. 3, pp. 504–511, Mar. 1998.

[28] P. Dimbylow, "FDTD calculations of the whole-body averaged SAR in an anatomically realistic voxel model of the human body from 1 MHz to 1 GHz," *Phys. Med. Biol.*, vol. 42, pp. 479–490, 1997.

[29] [Online]. Available: http://www.sam-phantom.com

[30] B. Hansson, "Development of SAR estimation formulas for RF exposure from base station antennas transmitting at 900 MHz, 1800 MHz, and 2140 MHz," Master's thesis, Uppsala Univ., Uppsala, Sweden, 2006.

[31] M. L. Strydom, "Assessing the specific absorption rate (SAR) in the human body in the near field of a base station antenna—a literature survey and discussion," EM Softw. Syst. S.A. (Pty) Ltd.Tech. Rep., 2007.

[32] M. J. van Wyk, M. Bingle, and F. J. C. Meyer, "Antenna modeling considerations for accurate SAR calculations in human phantoms in close proximity to GSM cellular base station antennas," *Bioelectromagnetics*, vol. 26, pp. 502–509, 2005.

[33] V. Kellerman, "Investigating the effect of accurate antenna modelling on the 10g peak-SAR value," private communication, 2006.

[34] C. Balanis, *Antenna Theory, Analysis and Design*. New York: Wiley, 1982.

[35] R. Cicchetti and A. Faraone, "Estimation of the peak power density in the vicinity of cellular and radio base station antennas," *IEEE Trans. Electromagn. Compat.*, vol. 46, no. 2, pp. 275–290, May 2004.
[36] S. Ilvonen, "Studying the accuracy of FDTD analysis for human exposure evaluation in the vicinity of a base station antenna," Helsinki Univ. Technol., Electromagn. Lab., Helsinki, Finland, and Nokia Corporation, Tech. Rep., 2007.
[37] A. Faraone, R. Y. Tay, K. Joyner, and Q. Balzano, "Estimation of the average power density in the vicinity of cellular base-station collinear array antennas," *IEEE Trans. Veh. Technol.*, vol. 49, no. 3, pp. 984–996, May 2000.
[38] R. A. Tell, "EME design and operation considerations for wireless antenna sites," Cell. Telecommun. Ind. Assoc.Tech. Rep., 1996.

Björn Thors received the M.Sc. degree in engineering physics from Uppsala University, Uppsala, Sweden, in 1996, and the Ph.D. degree in electromagnetic theory from the Royal Institute of Technology (KTH), Stockholm, Sweden, in 2003.

He spent the 2001–2002 academic year with The ElectroScience Laboratory, The Ohio State University, Columbus, as a Visiting Scholar, where he was engaged in the development of high-frequency methods for conformal antennas. From 2003 to 2005, he was a Research Associate at KTH. He is currently with Ericsson Research, Stockholm, where he is engaged in research on human exposure to radio frequency electromagnetic fields. His current research interests include electromagnetics, numerical and experimental techniques with applications in bioelectromagnetics, and dosimetric aspects of the interaction between electromagnetic fields and the human body.

Marie L. Strydom was born in Mpumalanga, South Africa. She received the B.Eng and M.Sc. degrees from the University of Stellenbosch, Stellenbosch, South Africa, in 1998 and 2003 respectively.

Since 2004, she has been actively involved in the field of computational electromagnetics, first at the University of Victoria, BC, Canada, where she researched the effects of high-Tesla MRI scanners on the fetus, and in 2006, as a Consultant to EMSS Software & Systems. Since 2007, she has been with CST GMBH, Darmstadt, Germany. Her current research interests include biomedical thermal effects of electromagnetic fields on the human body and general applications of computational electromagnetics.

Björn Hansson was born in Stockholm, Sweden, in 1982. He received the M.Sc. degree in engineering physics in 2006 from Uppsala University, Uppsala, Sweden, from where he also completed the Master's thesis.

Thereafter, he joined the Electromagnetic Field (EMF) Safety and Sustainability Department at Ericsson Research. His current research interests include EMF exposure from base station antennas, and specific absorption rate (SAR) testing of mobile communication devices.

Frans J. C. Meyer received the B.Eng degree in electronic engineering in 1988, the M.Eng. degree (*cum laude*) in 1991 in electronic engineering, and the Ph.D. degree in 1994 in numerical techniques in electromagnetic engineering, all from the University of Stellenbosch, Stellenbosch, South Africa.

He is the Co-Founder of EM Software & Systems, a company specializing in the development of commercial software products for the electromagnetic simulations market, including the well-established FEKO suite of software. Since 1995, when EMSS was founded, he was involved in bioelectromagnetic research and consulting work, first as a Principal Researcher and later as Head of a small research group. The research group focused on human exposure to mobile phones and later on human exposure to base station antennas. Currently, he is with EMSS Consulting, Stellenbosch, where he is engaged in research on mobile network compliance to international safety standards, which involves the development of numerical compliance software, field measurement projects, and training for RF workers.

Dr. Meyer has been a member of the Bioelectromagnetic Society for the past nine years.

Kimmo Kärkkäinen was born on February 1, 1973, in Kuopio, Finland. He received the M.Sc (Tech.), Lic.Sc. (Tech.), and D.Sc. (Tech.) degrees in electrical engineering from the Department of Electrical Engineering, Helsinki University of Technology (TKK), Espoo, Finland, in 1998, 2000, and 2003, respectively.

In 2000–2001, he was a Visiting Scientist in the Applied Electromagnetics Group, University of Victoria, Victoria, BC, Canada. In 2002–2004, he was a Teaching Scientist in the Electromagnetics Laboratory of TKK. He has been a Researcher and Project Manager at Nokia Research Center during 2004–2005 and Nokia Corporation during 2006–2007, participating in international standardization of electromagnetic field dosimetry. Currently, he is the Chief Executive Officer of Equal Dreams Ltd., Espoo.

Peter Zollman received the B.Sc. (Hons) degree in electrical and electronic engineering in 1979 from the University College of North Wales, Bangor, U.K.

From 1979 to 1983, he was with Racal Communications. From 1983 to 1990, he was with what is now Vodafone, where he was engaged in research on RF survey systems; coverage prediction, and on-frequency cellular repeaters. From 1990 to 1998, he was engaaged in research on global sysetm for mobile communications (GSM) handset-type approval for helping develop the associated ETSI standards and was the Project Manager at GSM Facilities Ltd. before chairing the GSM Association Certification Task Force. In 1998, he joined Vodafone UK's Advanced Development Group, which in 2001, became Vodafone Group R&D with interests in mobile telecommunications health and safety. He contributed to CENELEC base station electromagnetic field (EMF) standards, and is, currently, the Project Leader for IEC TC106 project team 62232 developing a global base station RF field/specificc absorption rate (SAR) standard; Chair of the U.K. Mobile Operators' Association Science Working Group; and, Chair of the GSM Association EMF Expert Panel.

Mr. Zollman is a Chartered Engineer and a Fellow of the Institute of Engineering and Technology.

Sami Ilvonen was born in Juuka, Finland, in 1975. He received the M.Sc. degree in electrical engineering from Helsinki University of Technology (TKK), Espoo, Finland, in 2000. He is currently working toward the D.Sc. degree as a Researcher in the Department of Radio Science and Engineering (TKK).

His current research interests include computational electromagnetics.

Christer Törnevik (M'98) received the M.Sc. degree in applied physics from the Linköping University, Linköping, Sweden, in 1986, and the Lic. (Tech.) degree in materials science from the Royal Institute of Technology, Stockholm, Sweden, in 1991.

He joined Ericsson in 1991, and has, since 1993, been involved in research and standardization activities related to radio frequency exposure from wireless communication equipment. He is currently the Head of a unit within Ericsson Research dealing with electromagnetic safety. He represents Ericsson on the Board of the Mobile Manufacturers Forum (MMF).